PHYSICAL REVIEW B VOLUME 18, NUMBER 7 1 OCTOBER 1978

Zero-temperature renormalization method for quantum systems. I. Ising model in a transverse field in one dimension

R. Jullien and P. Pfeuty
Laboratoire de Physique des Solides, Université Paris-Sud, Centre d'Orsay, 91405 Orsay, France

J. N. Fields
Department of Physics, Brookhaven National Laboratory, Upton, New York 11973

S. Doniach
Department of Applied Physics, Stanford University, Stanford, California 94305
(Received 6 March 1978)

A zero-temperature real-space renormalization-group method is presented and applied to the quantum Ising model with a transverse field in one dimension. The transition between the low-field and high-field regimes is studied. Magnetization components, spin correlation functions, and critical exponents are derived and checked against the exact results. It is shown that increasing the size of the blocks in the iterative procedure yields more accurate results, especially for the critical "magnetic" exponents near the transition.

I. INTRODUCTION

A new real-space renormalization-group method for quantum systems, introduced by Jafarey *et al.*,[1] has been used by Drell *et al.*[2] to study quantum fields on a lattice and by Jullien *et al.*[3] to study a model Hamiltonian for the Kondo lattice. Like the other methods[4] recently introduced for quantum spin systems, it is a block-spin method, but it emphasizes the ground-state properties of the system by working at $T=0$. The method consists of an iterative and approximate construction of the low-lying states of a quantum system. The lattice is split into blocks which are solved exactly. A given number of low-lying eigenstates are retained to write the interblock interaction, and the scheme is repeated until it converges to a "fixed point." This is, in a simpler case, similar to the work of Wilson[5] on the Kondo impurity problem. But Wilson used an "onion" scheme instead of using a multiplicative block method valid for translational-invariant problems.

The method is well suited for a number of problems where the nature of the ground state changes drastically at a critical value of one parameter. A typical example is the Ising model in a transverse field[6] where there is a transition from a low-field regime $h<h_c$, with a degenerate ground state, to a high-field regime $h>h_c$ with a singlet ground state. This model is studied here as a test of the method since it has been extensively studied by other methods and exactly solved in one dimension.[6] Jafarey *et al.*[1] treated the more simplified version of the method applied to the Ising model in a transverse field in one dimension; they worked with blocks of two sites and they retained only two levels at each iteration. In this case, the recursion relations are very simple and take analytical forms. The main physics of the transition is reproduced but there are some quantitative discrepancies concerning the location of the transition, the field dependence of the ground-state energy and the values of the critical indices near the transition. Particularly the index β for the longitudinal component of the magnetization below the transition is far away from the exact result: 0.40 instead of 0.125. Drell *et al.*[2] have already improved this estimate of β by use of some extensions of the method based on a variational procedure. Unfortunately, their technique yields an estimate for the location of the transition which is worse than that of Jafarey *et al.*[1] We have already presented another extension which consists of retaining many more levels at each step.[3] Both the location of the transition and the critical exponent for the gap after the transition are much improved by this method. Unfortunately we have not evaluated β in this method.

The purpose of the present paper is to present an alternative extension which consists of increasing the size of the blocks, but keeping always only two levels at each iteration. The advantage of keeping two levels is that the Hamiltonian can be written as a spin Hamiltonian at each iteration. As a direct consequence, the magnetization components and the spin correlation functions can be derived by use of spin recursion relations. In Sec. II the method is described. In Sec. III we present the renormalization-group trajectories and the fixed points, the location of the transition $(h/J)_c$, the calculated values of the ground-state energy and the energy gap between the ground-

state energy and the band of excited states. In Secs. IV and V the magnetization components and the correlation functions are calculated. The critical behavior of the transition close to $(h/J)_c$ is discussed in Sec. VI, where the various critical exponents are calculated, compared with exact results and tested with the scaling laws. A general discussion and conclusion is proposed in Sec. VII.

II. DESCRIPTION OF THE METHOD

The Ising model in a transverse field is described in one dimension for a chain with free ends by the following Hamiltonian:

$$H=-\left(J\sum_i S_i^x S_{i+1}^x+h\sum_i S_i^z\right). \tag{1}$$

We consider the limit of a large number N of spins. S_i^x and S_i^z are, for each site i, the usual spin-$\frac{1}{2}$ Pauli matrices:

$$S^x=\begin{pmatrix}0&1\\1&0\end{pmatrix},\quad S^z=\begin{pmatrix}1&0\\0&-1\end{pmatrix}. \tag{2}$$

Our method uses an iterative procedure which yields the following form for the Hamiltonian at the iteration n:

$$H^{(n)}=-\sum_i (J^{(n)}S_i^{x(n)}S_{i+1}^{x(n)}+h^{(n)}S_i^{z(n)})+C^{(n)}\sum_i I_i^{(n)}, \tag{3}$$

where $I_i^{(n)}$ is, at step n, a single-site 2×2 identity matrix. We start at $n=0$ with the initial spins entering (1) and the parameters

$$J^{(0)}=J,\quad h^{(0)}=h,\quad C^{(0)}=0. \tag{4}$$

At the iteration n, we divide the chain into adjacent blocks of n_s sites. We then use new indices (j,p): j being the label of the block, and p $(1\leq p\leq n_s)$ being the label of the spin in the block. We write $H^{(n)}$ under the form

$$H^{(n)}=\sum_j\left(H_j^{(n)}+H_{j,j+1}^{(n)}+C^{(n)}\sum_{p=1,\ldots,n_s} I_{j,p}^{(n)}\right), \tag{5}$$

where $H_j^{(n)}$ is an intrablock Hamiltonian:

$$H_j^{(n)}=-J^{(n)}\sum_{p=1,\ldots,n_s-1} S_{j,p}^{x(n)}S_{j,p+1}^{x(n)}-h^{(n)}\sum_{p=1,\ldots,n_s} S_{j,p}^{z(n)} \tag{6}$$

and where $H_{j,j+1}^{(n)}$ is the interblock interaction:

$$H_{j,j+1}^{(n)}=-J^{(n)}S_{j,n_s}^{x(n)}S_{j+1,1}^{x(n)}. \tag{7}$$

First, we solve $H_j^{(n)}$ exactly in the space ϵ_j of dimensionality 2^{n_s} generated by the basis vectors $|\epsilon_1,\epsilon_2,\ldots,\epsilon_p,\ldots,\epsilon_{n_s}\rangle$, where ϵ_p takes the value $+1$ or -1 corresponding to the eigenstates of $S_{j,p}^{z(n)}$ in the block. This diagonalization can be simplified by observing that H_j, acting on a basis vector, does not change the parity of the total number of (+) or (−) signs. Thus, we diagonalize H_j separately in the two different subspaces ϵ_j^+ and ϵ_j^- of dimensionality 2^{n_s-1} generated, respectively, by the basis vectors having an even and odd number of minus signs.

After the diagonalization of $H_j^{(n)}$, we retain only the lowest energy states of each subspaces $\epsilon_j^{\pm}$ which we designate by $|+\rangle^{(n+1)}$ and $|-\rangle^{(n+1)}$, the corresponding eigenvalues being $E_+^{(n+1)}$ and $E_-^{(n+1)}$, respectively. We write

$$\begin{aligned}|+\rangle^{(n+1)}&=\sum{}^{+}\lambda^{+(n)}_{\epsilon_1,\ldots,\epsilon_p,\ldots,\epsilon_{n_s}}\\&\quad\times|\epsilon_1,\ldots,\epsilon_p,\ldots,\epsilon_{n_s}\rangle,\\|-\rangle^{(n+1)}&=\sum{}^{-}\lambda^{-(n)}_{\epsilon_1,\ldots,\epsilon_p,\ldots,\epsilon_{n_s}}\\&\quad\times|\epsilon_1,\ldots,\epsilon_p,\ldots,\epsilon_{n_s}\rangle,\end{aligned} \tag{8}$$

where $\sum^+$ and $\sum^-$ are summation signs restricted to the subspaces ϵ_j^+ and ϵ_j^-, respectively. The coordinates $\lambda^{\pm(n)}_{\epsilon_1,\ldots,\epsilon_p,\ldots,\epsilon_{n_s}}$ and the eigenvalues $E_{\pm}^{(n+1)}$ are determined by machine as a function of the parameters $h^{(n)}$ and $J^{(n)}$ at each iteration. Our choice for ϵ_j^+ and ϵ_j^- yield $E_+^{(n+1)}<E_-^{(n+1)}$; we observe that no first excited state of one space lies below the ground state of the other so that these $E_+^{(n+1)}$ and $E_-^{(n+1)}$ levels are always the two lowest levels of the whole spectrum of $H_j^{(n)}$.

We then introduce a new set of spin operators $S_j^{x(n+1)}$ attached to each block j, the eigenstates of $S_j^{z(n+1)}$ being precisely $|+\rangle^{(n+1)}$ and $|-\rangle^{(n+1)}$. $H_j^{(n)}$ is rewritten in the new spin representation as

$$H_j^{(n)}=-h^{(n+1)}S_j^{z(n+1)}+\tfrac{1}{2}(E_+^{(n+1)}+E_-^{(n+1)})I_j^{(n+1)} \tag{9}$$

with

$$h^{(n+1)}=\tfrac{1}{2}(E_-^{(n+1)}-E_+^{(n+1)}). \tag{10}$$

Taking the matrix elements of the old spin $S_{j,p}^{x(n)}$ between the block states $|+\rangle^{(n+1)}$ and $|-\rangle^{(n+1)}$, we obtain the following spin recursion relation:

$$S_{j,p}^{x(n)}=\xi_p^{x(n)}S_j^{x(n+1)} \tag{11}$$

with

$$\xi_p^{x(n)}=\sum{}^{+}\lambda^{+(n)}_{\epsilon_1,\ldots,\epsilon_p,\ldots,\epsilon_{n_s}}\lambda^{-(n)}_{\epsilon_1,\ldots,-\epsilon_p,\ldots,\epsilon_{n_s}}. \tag{12}$$

The quantities $\xi_p^{x(n)}$, functions of $h^{(n)}$ and $J^{(n)}$, can be evaluated at each iteration; for symmetry reasons, we observe that $\xi_{n_s-p+1}^{x(n)}=\xi_p^{x(n)}$ and especially $\xi_{n_s}^{x(n)}=\xi_1^{x(n)}$. The relation (11) allows us to rewrite the interblock Hamiltonian $H_{j,j+1}^{(n)}$, in terms of the new spins

$$H_{j,j+1}^{(n)}=-J^{(n+1)}S_j^{x(n+1)}S_{j+1}^{x(n+1)} \tag{13}$$

with

$$J^{(n+1)} = (\xi_1^{x(n)})^2 J^{(n)} . \tag{14}$$

Then, inserting (9) and (13) into (5) we recover the same form (3) at iteration $n+1$ with the new constant:

$$C^{(n+1)} = n_s C^{(n)} + \tfrac{1}{2}(E_+^{(n+1)} + E_-^{(n+1)}) . \tag{15}$$

The recursion relations (10), (14), (15), along with the initial condition (4), define a renormalization-group transformation. The parameter $h^{(n)}$ provides information on the splitting of the two lowest levels of the system and Eq. (15) may be used to find the absolute value of the energy per site E_0/N of the ground state in the limit $N \to \infty$ through the relation

$$(E_0/N)_{N\to\infty} = \lim_{n\to\infty} (C^{(n)}/n_s^n) \tag{16}$$

III. FIXED POINTS OF THE RENORMALIZATION-GROUP TRANSFORMATION AND DETERMINATION OF THE LOWEST-ENERGY LEVELS (GROUND-STATE ENERGY AND ENERGY GAP)

We have done the calculation for $n_s = 2, 3, 4, 5, 6, 7$. The general features of the transition already described in the simplest case $n_s = 2^{(1)}$ are recovered:

(i) for h/J smaller than a critical value $(h/J)_c$, $h^{(n)} \to 0$ while $J^{(n)} \to J^\infty \neq 0$ when $n \to \infty$, so that *the ground state is a doublet*. The renormalization-group trajectory converges to a fixed point corresponding to a simple Ising chain (without applied field) with a coupling constant equal to J^∞.

(ii) For h/J greater than $(h/J)_c$, when $n \to \infty$ $h^{(n)} \to h^\infty \neq 0$ while $J^{(n)} \to 0$ so that the ground state is *a singlet* separated by a gap $\Delta = 2h^\infty$ from the first excited states. The renormalization-group trajectory converges to a fixed point corresponding to a chain of independent spins with an applied field in the z direction equal to h^∞.

In the one-parameter space h/J, $(h/J)_c$ is an unstable fixed point separating two stable fixed points $h/J = 0$ and $h/J = \infty$. In the two parameters space h, J, there are two fixed lines $h = 0$ and $J = 0$ corresponding to the two fixed-point Hamiltonians. (In fact the apparent marginality of these fixed lines is only due to the fact that h/J is the true physical parameter, it follows then that h^∞/J and J^∞/J are only functions of h/J.) Figure 1 gives the plot of J^∞/J (below the transition) and h^∞/J (above the transition) as a function of h/J. We observe that $h^\infty/J = \Delta/2J$ becomes more and more linear when n_s increases and follows fairly well the exact relation[6]

$$\Delta = 2(h - J) \tag{17}$$

represented by the dashed line in Fig. 1. This has been made more precise by extracting the critical exponent s for the gap defined just above the transition by

$$\Delta \sim (h - h_c)^s . \tag{18}$$

The results for s are given in Table I. We observe that s increases and tends slowly to one when n_s increases.

We observe also that J^∞/J becomes close to the parabolic relation

$$J^\infty = J[1 - (h/J)^2] \tag{19}$$

which is represented by the dashed curve in Fig. 1. This result will be explained at the end of the paper when we establish the link between J^∞/J and the end-to-end x-x correlation function.[7] The location of the transition $(h/J)_c$ tends to the exact value $(h/J)_c = 1$, when n_s increases, as shown in Table I.

We have calculated also the ground-state energy per site E_0/N and we have plotted, in Fig. 2, its second derivative with respect to the field, which represents the z magnetic susceptibility $\chi_z = \partial\langle 0|S^z|0\rangle/\partial h$, as a function of h/J. The logarithmic divergence which appears at the transition in the exact results (dashed curve) becomes quite well reproduced in our calculation for large n_s values. This is a real improvement over the simplest case $n_s = 2$ where there is no peak but only a change of slope at the transition. The same kind of improvement was obtained by Drell *et al.*[2] with their variational renormalization-group method.

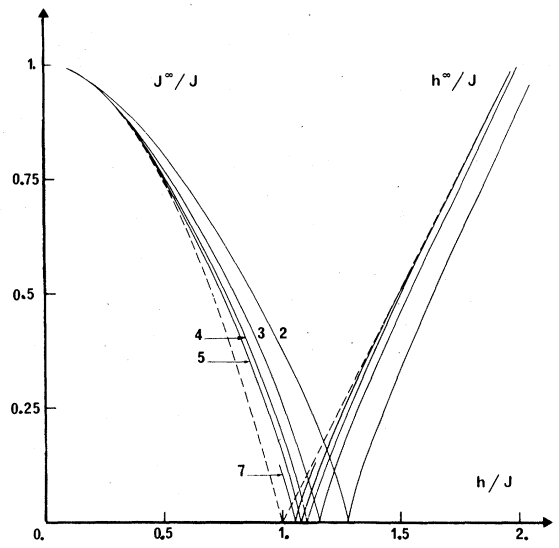

FIG. 1. Plot of J^∞/J (below the transition) and h^∞/J (above the transition) as a function of h/J for different n_s values. The exact results are represented by the dashed curve.

TABLE I. Results for the critical field and the critical exponents obtained by this approach (with $n_s = 2, 3, \ldots, 7$) compared with the exact values (Ref. 6).

n_s	2	3	4	5	6	7	Exact
$(h/J)_c$	1.276 75	1.154 70	1.105 68	1.079 71	1.063 77	1.053 05	1
s	0.805	0.82	0.835	0.845	0.855	0.86	1
ν	1.47	1.31	1.24	1.20	1.18	1.16	1
z	0.55	0.63	0.675	0.705	0.725	0.74	1
νz	0.81	0.83	0.84	0.845	0.855	0.86	1
β^*	0.40	0.40	0.40	0.40	0.405	0.405	0.5
β	0.40	0.18	0.185	0.155	0.155	0.145	0.125
η_x	0.55	0.29	0.32	0.29	0.30	0.275	0.25
$2d_x$	0.55	0.29	0.32	0.275	0.285	0.27	0.25
$2\beta/\nu$	0.54	0.275	0.30	0.26	0.265	0.25	0.25
η_y	1.65	1.55	1.67	1.68	1.74	1.75	2.25
$2d_y$	1.65	1.55	1.67	1.68	1.74	1.75	2.25
$\eta_x + 2z$	1.65	1.55	1.67	1.69	1.75	1.75	2.25
η_z	2.21	1.79	1.92	1.86	1.91	1.89	2
$2d_z$	2.20	1.78	1.92	1.86	1.91	1.89	2

Let us now complete this study by looking at the magnetization components and correlation functions.

IV. MAGNETIZATION COMPONENTS

The x, y, and z components of the magnetization are given by the expectation values $\langle 0|S_i^x|0\rangle$, $\langle 0|S_i^y|0\rangle$, $\langle 0|S_i^z|0\rangle$, where $|0\rangle$ is the ground state of the spin system. For an infinite chain with free ends these quantities are independent of i when i is far from the edges. Suppose we stop the iteration scheme at step n. The original chain made of superblocks of n_s^n sites is then replaced by a chain of spins $\vec{S}_j^{(n)}$, each superblock being represented by a unique spin. By using the spin recursion relation (11) we obtain for the x component

$$\langle S_i^x \rangle = \xi_{p_0}^{x(0)} \xi_{p_1}^{x(1)} \cdots \xi_{p_{n-1}}^{x(n-1)} \langle S_j^{x(n)} \rangle . \tag{20}$$

The indices $p_0, p_1, \ldots, p_{n-1}$ depend on the location of $\vec{S}_i$ in the superblock of index j.

Similar relations can be derived for the other components. By taking the matrix elements of $S_{j,p}^{x(n)}$ and $S_{j,p}^{z(n)}$ between the block states $|+\rangle^{(n+1)}$ and $|-\rangle^{(n+1)}$, we obtain the following recursion relations:

$$S_{j,p}^{y(n)} = \xi_p^{y(n)} S_j^{y(n+1)} , \tag{21a}$$

$$S_{j,p}^{z(n)} = \zeta_p^{z(n)} I_j^{(n+1)} + \xi_p^{z(n)} S_j^{z(n+1)} , \tag{21b}$$

where

$$\xi_p^{y(n)} = \sum\nolimits^{+} \epsilon_p \lambda^{+(n)}_{\epsilon_1, \ldots, \epsilon_p, \ldots, \epsilon_{n_s}} \lambda^{-(n)}_{\epsilon_1, \ldots, -\epsilon_p, \ldots, \epsilon_{n_s}} \tag{22}$$

and

$$\zeta_p^{z(n)} = \tfrac{1}{2}(\eta_p^{+(n)} + \eta_p^{-(n)}) , \tag{23a}$$

$$\xi_p^{z(n)} = \tfrac{1}{2}(\eta_p^{+(n)} - \eta_p^{-(n)}) \tag{23b}$$

with

$$\eta_p^{\pm(n)} = \sum\nolimits^{\pm} \epsilon_p (\lambda^{\pm(n)}_{\epsilon_1, \ldots, \epsilon_p, \ldots, \epsilon_{n_s}})^2 . \tag{23c}$$

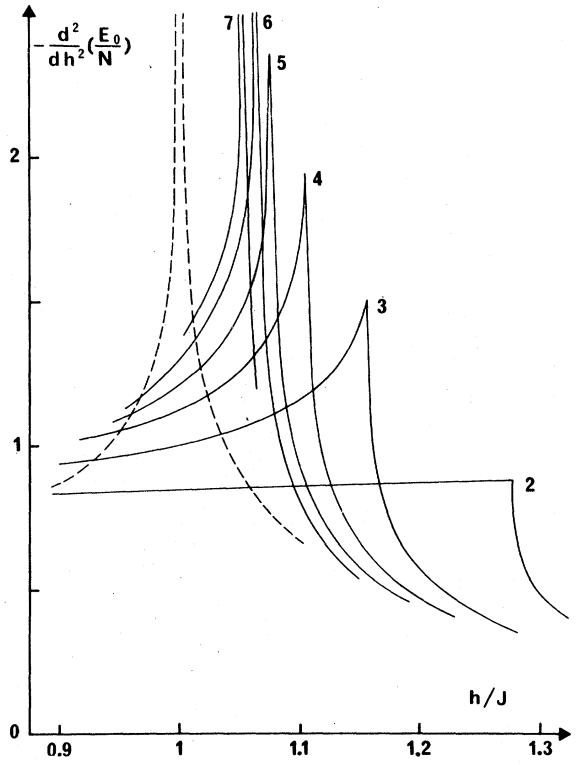

FIG. 2. Plot of $-\partial^2/\partial h^2 (E_0/N)$ as a function of h/J for different n_s values. The exact result is represented by the dashed curve.

Relations (21a) and (21b) can be used to obtain

$$\langle S_i^y \rangle = \xi_{p_0}^{y(0)} \xi_{p_1}^{y(1)} \cdots \xi_{p_{n-1}}^{y(n-1)} \langle S_j^{y(n)} \rangle , \tag{24a}$$

$$\langle S_i^z \rangle = Z_{p_0,\ldots,p_{n-1}}^{0,n-1} + \xi_{p_0}^{z(0)} \xi_{p_1}^{z(1)} \cdots \xi_{p_{n-1}}^{z(n-1)} \langle S_j^{z(n)} \rangle , \tag{24b}$$

where for $m > n$ we define

$$Z_{p_n,\ldots,p_m}^{n,m} = \xi_{p_n}^{z(n)} + \xi_{p_n}^{z(n)} \xi_{p_{n+1}}^{z(n+1)} + \cdots + \xi_{p_n}^{z(n)} \times \xi_{p_{n+1}}^{z(n+1)} \cdots \xi_{p_{m-1}}^{z(m-1)} \xi_{p_m}^{z(m)} . \tag{25}$$

If n is sufficiently large, the Hamiltonian goes to a fixed-point Hamiltonian described in Sec. III:

(i) For $h/J < (h/J)_c$ we obtain the Ising chain in the x direction, thus $\langle S^{x(n)} \rangle = \pm 1$ while $\langle S^{y(n)} \rangle = \langle S^{z(n)} \rangle = 0$. In principle we cannot distinguish between (+) or (−) for $\langle S^{x(n)} \rangle$ since there is no applied field in the x direction.[8]

(ii) For $h/J > (h/J)_c$ we obtain the free-spin chain in a positive z field, thus $\langle S^{x(n)} \rangle = \langle S^{y(n)} \rangle = 0$ while $\langle S^{z(n)} \rangle = +1$.

In addition, since $Z_{p_0,\ldots,p_{n-1}}^{0,n-1}$ must converge when $n \to \infty$, the cumulative infinite product $\xi_{p_0}^{z(0)} \xi_{p_1}^{z(1)} \cdots \xi_{p_n}^{z(n)} \cdots$ tends to zero when $n \to \infty$.

In conclusion

$$\langle S_i^x \rangle = \begin{cases} \lim_{n\to\infty} \xi_{p_0}^{x(0)} \xi_{p_1}^{x(1)} \cdots \xi_{p_m}^{x(n)} & \text{for } h/J < (h/J)_c , \quad (26a) \\ 0 \quad \text{for } h/J > (h/J)_c & (26b) \end{cases}$$

and

$$\langle S_i^y \rangle = 0 \quad \text{everywhere} , \tag{27}$$

$$\langle S_i^z \rangle = \lim_{n\to\infty} Z_{p_0,\ldots,p_n}^{0,n} \quad \text{everywhere} . \tag{28}$$

In these formulas the result depends on the set of the $p_0, \ldots, p_n$ values and thus on the location of the spin $\tilde{S}_i$ in the original chain. This dependence is an artifact of our approximate renormalization-group method. It is due to the way the division in blocks is made. In the renormalization procedure described in Sec. II, the spins at the edges of a block are not correctly included in the new approximate ground state. Thus we would make an error by taking the p_i equal or close to the values 1 or n_s. The best way to estimate the magnetization components is then to consider, at each step, a spin in the middle (or close to the middle, if n_s is even) of the block. So we expect that the x and z magnetization components μ_x and μ_z are well represented by the following quantities:

$$\mu_x = \lim_{n\to\infty} \xi_{p_0}^{x(0)} \xi_{p_0}^{x(1)} \cdots \xi_{p_0}^{x(n)} \quad \text{when } h/J < (h/J)_c , \tag{29}$$

$$\mu_z = \lim_{n\to\infty} Z_{p_0,p_0\cdots p_0}^{0,n} , \tag{30}$$

where p_0 is always the same and is $\frac{1}{2}(n_s+1)$ for n_s odd and $\frac{1}{2}n_s$ (or the symmetrical value $\frac{1}{2}n_s+1$) for n_s even. One can understand that the odd values of n_s are more interesting to evaluate μ_x and μ_z due to the peculiar situation of the site $\frac{1}{2}(n_s+1)$ just on the middle of the block.

These quantities have been evaluated through our recursion scheme. μ_x and μ_z are plotted as a function of h/J in Fig. 3(a) and 3(b) for $n_s = 2, 3, 5$. The exact results[6] for the magnetization are represented by the dashed curves. Also, in inset of Fig. 3(b) we compare for $n_s = 5$ the calculation of μ_z by formula (30) and by taking the first derivative of the approximate ground-state energy per site: $-\partial(E_0/N)/\partial h$. This second procedure is less accurate.

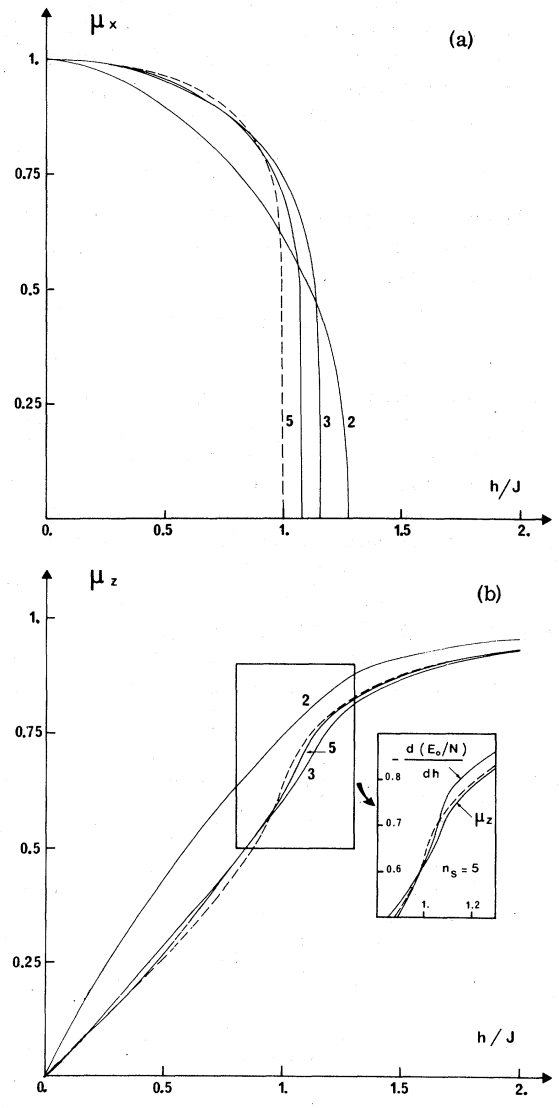

FIG. 3. Plot of the x component (a) and z component (b) of the magnetization as a function of h/J for $n_s = 2, 3, 5$. The exact results are represented by the dashed curves. In inset of (b) is shown for $n_s = 5$ the results for $-\partial/\partial h(E_0/N)$.

In the case of the x component the results can be made quantitatively precise by extracting the critical exponent β defined just below the transition by

$$\mu_x \sim [\,(h/J)_c - h/J\,]^{\beta}\,. \tag{31}$$

The results for β are reported in Table I. We recall that the exact result is $\beta = 0.125$.[6] The bad value $\beta = 0.40$ obtained for $n_s = 2$ is already greatly improved by considering blocks of three sites. Also, we can see that increasing n_s by 1 from an odd value does not improve β. This confirms the advantage of taking n_s odd to calculate the magnetization. For $n_s = 7$ we obtain $\beta = 0.145$ (15% error) which is remarkably near the exact value.

In Table I we compare the results for β with the results for the "wrong" exponent β^*, β^* being the critical exponent of the cumulative product taken always at the block edges:

$$\lim_{n\to\infty} (\xi_1^{x(0)}, \ldots, \xi_1^{x(n)}) \sim [(h/J)_c - h/J]^{\beta^*}\,. \tag{32}$$

Note that, through relation (14), this product is the square root of J^{∞}/J. Thus β^* is also the half of the critical exponent for J^{∞}/J.

V. CORRELATION FUNCTIONS

Let us consider now the x-x, y-y, and z-z correlation functions given by $\langle 0|S_i^x S_{i'}^x|0\rangle$, $\langle 0|S_i^y S_{i'}^y|0\rangle$, $\langle 0|S_i^z S_{i'}^z|0\rangle$. At the beginning we can transform the spins $\vec{S}_i$ and $\vec{S}_{i'}$ with the recursion relations (11), (21a), and (21b) but at a given step, which depends on the distance between the spins and the way the blocks are defined, we obtain two spins in the same block and we can no longer use (11), (21a), and (21b). Thus, at a given step n, we need to express the product operators $S_{j,p}^{\alpha(n)} S_{j,p'}^{\alpha(n)}$ $(\alpha = x, y, z)$ where p and p' are two different sites of a block j as a function of the spin operators $S_j^{\alpha(n+1)}$ of the block.

We obtain

$$S_{j,p}^{\alpha(n)} S_{j,p'}^{\alpha(n)} = \zeta_{pp'}^{\alpha(n)} I_j^{(n+1)} + \xi_{pp'}^{\alpha(n)} S_j^{\alpha(n+1)} \tag{33}$$

with

$$\zeta_{pp'}^{\alpha(n)} = \frac{1}{2}(\eta_{pp'}^{+\alpha(n)} + \eta_{pp'}^{-\alpha(n)})\,, \tag{34a}$$

$$\xi_{pp'}^{\alpha(n)} = \frac{1}{2}(\eta_{pp'}^{+\alpha(n)} - \eta_{pp'}^{-\alpha(n)})\,, \tag{34b}$$

and

$$\eta_{pp'}^{\pm x(n)} = \sum{}^{\pm} \lambda_{\epsilon_1,\ldots,\epsilon_p,\epsilon_{p'},\ldots,\epsilon_{n_s}}^{\pm(n)} \times \lambda_{\epsilon_1,\ldots,-\epsilon_p,-\epsilon_{p'},\ldots,\epsilon_{n_s}}^{\pm(n)}\,, \tag{35a}$$

$$\eta_{pp'}^{\pm y(n)} = -\sum{}^{\pm} \epsilon_p \epsilon_{p'} \lambda_{\epsilon_1,\ldots,\epsilon_p,\epsilon_{p'},\ldots,\epsilon_{n_s}}^{\pm(n)} \times \lambda_{\epsilon_1,\ldots,-\epsilon_p,-\epsilon_{p'},\ldots,\epsilon_{n_s}}^{\pm(n)}\,, \tag{35b}$$

$$\eta_{pp'}^{\pm z(n)} = \sum{}^{\pm} \epsilon_p \epsilon_{p'} (\lambda_{\epsilon_1,\ldots,\epsilon_p,\epsilon_{p'},\ldots,\epsilon_{n_s}}^{\pm(n)})^2\,. \tag{35c}$$

In the case of the short-range correlation functions the relation (33) has to be applied at the beginning and we obtain

$$\rho_\alpha(1) = \langle S_p^\alpha S_{p+1}^\alpha \rangle = \zeta_{p,p+1}^{\alpha(0)} + \xi_{p,p+1}^{\alpha(0)} \lim_{n\to\infty} Z_{p_1,\ldots,p_n}^{1,n}\,. \tag{36}$$

The best way to calculate these quantities is to choose $p = p_0$ and $p_1 = p_2 = \cdots = p_n = p_0$, where $p_0 = \frac{1}{2}(n_s + 1)$ for n_s odd and $p_0 = \frac{1}{2} n_s$ for n_s even. Here, the most interesting situation is given for even values of n_s where p_0 and $p_0 + 1$ take the symmetrical values $\frac{1}{2} n_s$ and $\frac{1}{2} n_s + 1$.

The results for $\rho_x(1), \rho_y(1), \rho_z(1)$ are reported in Figs. 4(a)–4(c) for $n_s = 2, 4, 6$ and compared with the exact results of Ref. 6.[9]

Let us consider now the case where the spins $\vec{S}_i$ and $\vec{S}_{i'}$ are situated in two different adjacent superblocks j and $j+1$ represented after n iterations by the two adjacent spins $\vec{S}_j^{(n)}$ and $\vec{S}_{j+1}^{(n)}$. We obtain

$$\langle S_i^x S_{i'}^x \rangle = (\xi_{p_0}^{x(0)} \cdots \xi_{p_{n-1}}^{x(n-1)})(\xi_{p_0'}^{x(0)} \cdots \xi_{p_{n-1}'}^{x(n-1)}) \times (\zeta_{p_n,p_n'}^{x(n)} + \xi_{p_n,p_n'}^{x(n)} \lim_{m\to\infty} Z_{p_{n+1},\ldots,p_m'}^{n+1,m})\,. \tag{37}$$

A similar expression is obtained for $\langle S_i^y S_{i'}^y \rangle$ by changing x into y. An expression much more complicated and not reproduced here can also be obtained for $\langle S_i^z S_{i'}^z \rangle$.

On this formula we see that we obtain the same result if $\vec{S}_i$ has a given place in the superblock j or the symmetrical place with respect to the center of the block. This pseudoperiodicity of the correlation functions is again an artifact of the method. The best choice is to consider $\vec{S}_i$ and $\vec{S}_{i'}$ at the centers, or near the centers of the two adjacent superblocks and by taking then $p_0 = \cdots p_{n-1} = p_0' = \cdots = p_{n+1}^r = p_{n+1}'' = \cdots = p_m'' = \frac{1}{2} n_s$ (or $\frac{1}{2} n_s + 1$) for n_s even, $\frac{1}{2}(n_s + 1)$ for n_s odd and $p_n' = p_n + 1$ with $p_n = n_s$ for n_s even and $\frac{1}{2}(n_s + 1)$ for n_s odd. The distance between the two spins is then $R = n_s^n$. This situation is sketched for $n_s = 4$ and $n_s = 2$ in Fig. 5. Thus the method gives a good approximation for the correlation functions $\rho_\alpha(R)$ $(\alpha = x, y, z)$ for distances $R = 1, n_s, n_s^2, \ldots, n_s^n$, etc. Note that when $n \to \infty$ the above formula and the corresponding formulas for y and z give the square of the corresponding magnetization component as it is expected for long-range correlation functions. We have reported in the case $n_s = 6$ the results for $\rho_x(R), \rho_y(R), \rho_z(R)$, as a function of $\log R = n \log n_s$ for two values of h/J just below and just above the transition (Fig. 6).

From exact results[6,10] and scaling arguments ρ_x, ρ_y, and ρ_z must behave when h/J is close to

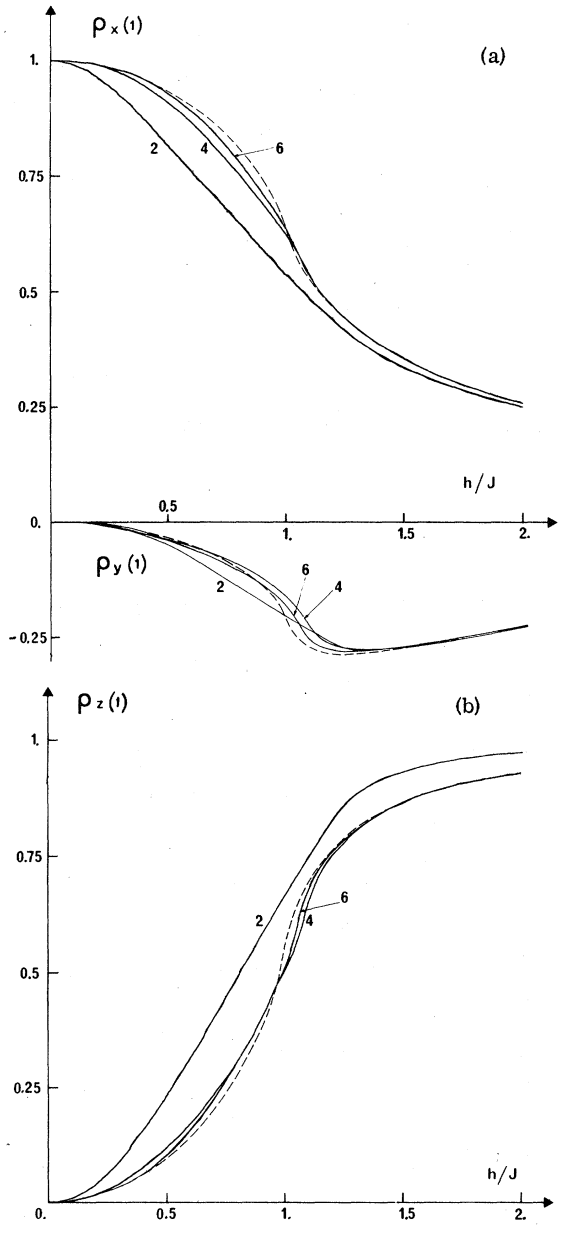

FIG. 4. Plot of the short-range correlation functions ρ_x (1) (a), ρ_y (1) (b), ρ_z (1) (c) as a function of h/J for $n_s = 2, 4, 6$. The exact results are represented by the dashed curves.

$(h/J)_c$ like

$$\rho_x = \mu_x^2 + (a_x/R^{n_x})F_x(R/R_c)\,, \tag{38}$$

$$\rho_y = (a_y/R^{n_y})F_y(R/R_c)\,, \tag{39}$$

$$\rho_z = \mu_z^2 + (a_z/R^{n_z})F_z(R/R_c)\,, \tag{40}$$

where R_c is the correlation length and varies like $[h/J - (h/J)_c]^{-\nu}$ and where $\eta_x = \frac{1}{4}$, $\eta_y = \frac{9}{4}$, $\eta_z = 2$ and if

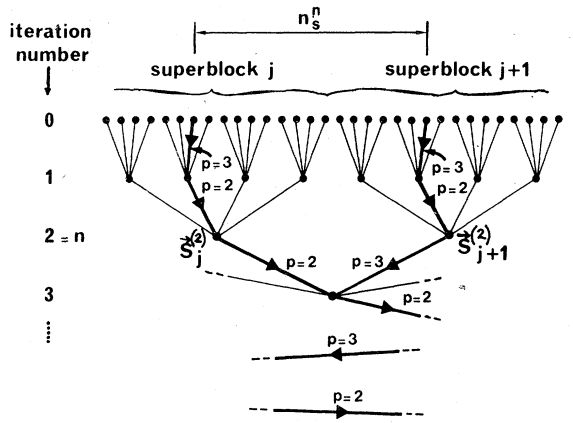

FIG. 5. Sketch of the calculation of ρ_α (16) in the case $n_s = 4$, $n = 2$. The thick lines show the spin recursions used.

we choose for instance $h/J > (h/J)_c$

$$F_x(u) \sim \frac{e^{-u}}{u^{1/4}}, \quad u \to \infty\,, \tag{41}$$

$$F_y(u) \sim \frac{e^{-u}}{u^{-3/4}}, \quad u \to \infty\,, \tag{42}$$

$$F_z(u) \sim e^{-u}(1 + u^{-1}), \quad u \to \infty\,, \tag{43}$$

for $u \to 0$,

$$F_x(u) = F_y(u) = F_z(u) = 1\,. \tag{44}$$

a_x, a_y, a_z are adequate constants.

For comparison we have plotted $\log(\rho_x - \mu_x^2)$ as a function of $\log R$ in Fig. 7 (for $n_s = 6$) for h/J values near $(h/J)_c$. We observe a linear behavior for not too large R and a departure from this linear behavior for $R > R_c$, where R_c is a measure of the correlation length. When h goes to h_c, R_c becomes larger and the linear region (the power-law behavior for ρ_x, ρ_y, ρ_z) increases and thus η_x can be measured and is equal to 0.30 which is near the exact value 0.25. The same has been done for ρ_y and ρ_z and the values of η_x, η_y, η_z are tabulated in Table I for $n_s = 2, 3, 4, 5, 6, 7$. We shall discuss these results in more detail in Sec. VI.

The scaling law for ρ_x has been checked. We have plotted in Fig. 8 $\log F_x$ as a function of $\log(R/R_c)$ for various values of h/J and all the points fall on the same curve. We should mention that $F(R/R_c)$ is not the same function for $h/J > (h/J)_c$ and for $h/J < (h/J)_c$. We did not check the function $F_x(u)$ versus the predicted theoretical form given by Eq. (41).

We want to mention here that the end-to-end x-x correlation function for the infinite chain is given by

$$\rho_x^{ee} = (\lim \xi_1^{x(0)} \xi_1^{x(1)} \cdots \xi_1^{x(n)})^2 = J^\infty/J\,. \tag{45}$$

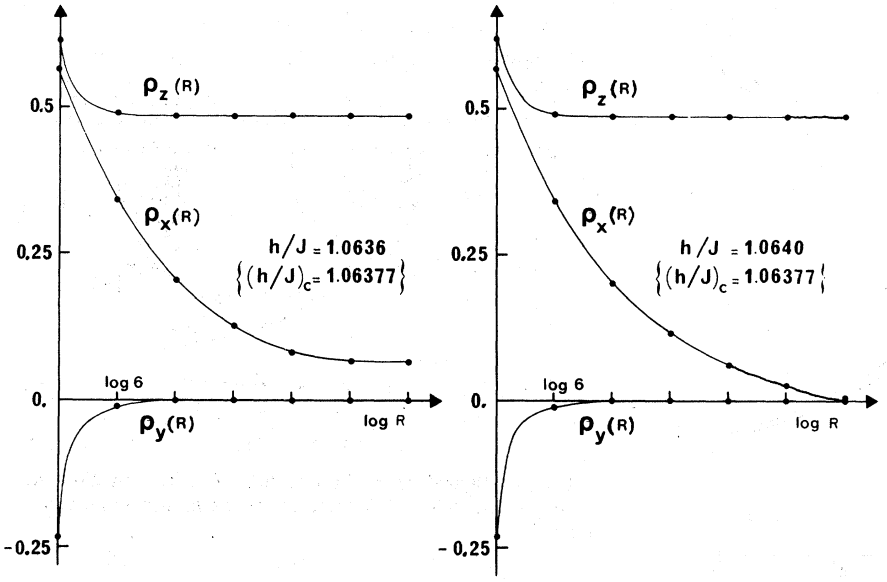

FIG. 6. Plot of the correlation functions $\rho_x(R)$, $\rho_y(R)$, $\rho_z(R)$ as a function of log R for $n_s = 6$ and two values of h/J just below and just above the transition.

The results for the end-to-end correlation function are completely different (due to edge effects) from those for the "bulk" long-range correlation function given by the square of the magnetization. The exact result[6] for ρ_x^{ee} is $\rho_x^{ee} = 1 - (h/J)^2$ which is the parabola reported by the dashed curve in Fig. 1. We observe that $\rho_x^{ee} = J^\infty/J$ tends to the exact value when n_s increases and at the same time β^* tends (very slowly) to 0.5 (Table I).

VI. CRITICAL BEHAVIOR

As first suggested[11] and then proved[12], there is a rigorous equivalence of the ground-state singularities of the one-dimensional Ising model in a transverse field to the singularities of the two-dimensional Ising model. The critical behavior of the Ising model in a transverse field close to the critical field $(h/J)_c$ is strictly equivalent to the critical behavior of the Ising model in two dimensions[13], close to T_c. We shall first discuss the "thermal exponents" z, ν, and s and later the "magnetic" exponents β, η_x, η_y, and η_z.

The exponent ν tells how the correlation length R_c diverges

$$R_c \sim [h/J - (h/J)_c]^{-\nu} . \tag{46}$$

It could be obtained from the analysis of $\rho_x(R)$ close to the critical field but a simpler and more elegant way is to extract ν directly from the recursion relations (10) and (14) which give the recursion relation for $h^{(n)}/J^{(n)}$. This recursion relation can be linearized for $h^{(n)}/J^{(n)}$ close to the fixed point $(h/J)_c$ to give

$$\frac{h^{(n+1)}}{J^{(n+1)}} - \left(\frac{h}{J}\right)_c = n_s^y \left(\frac{h^{(n)}}{J^{(n)}} - \left(\frac{h}{J}\right)_c\right) \tag{47}$$

and by simple scaling arguments we extract

$$\nu = 1/y . \tag{48}$$

For $n_s = 2$, ν can be obtained by hand. For larger values of n_s the determination of ν is done with the help of the computer. The values of ν are

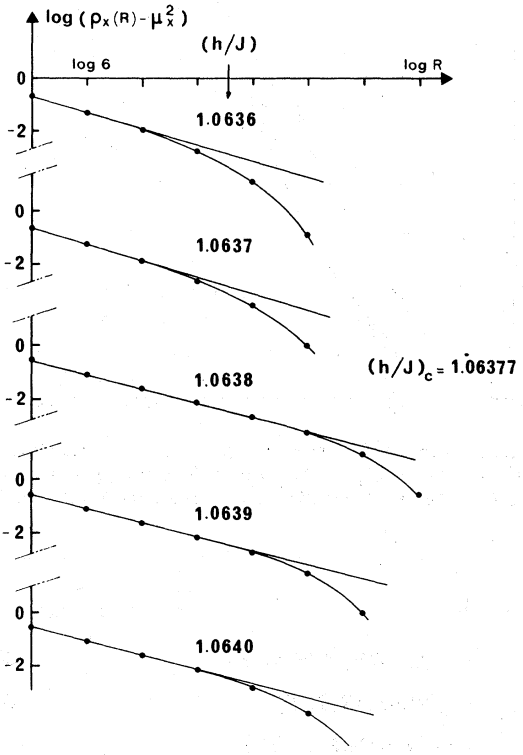

FIG. 7. Plot of log $[\rho_x(R) - \mu_x^2]$ as a function of $\log_{10} R$ for $n_s = 6$ and various values of h/J near the transition.

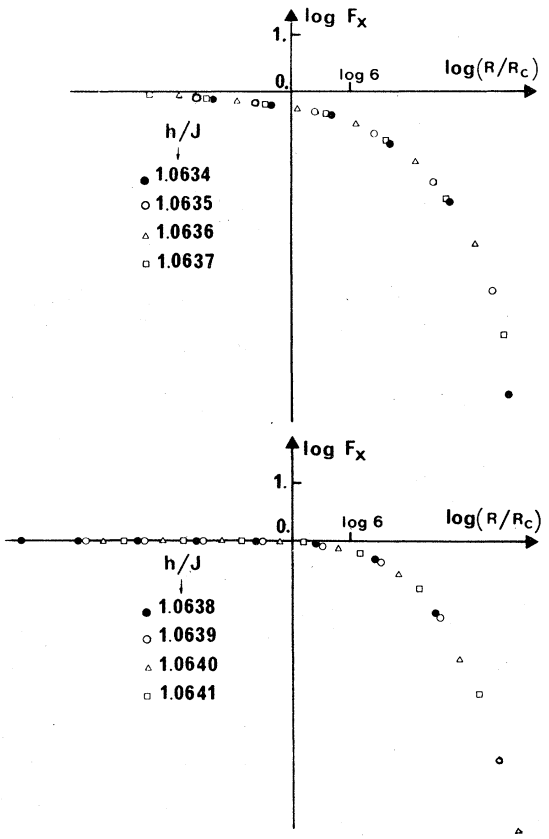

FIG. 8. Plot of the logarithm of the function F_x defined by relation (38) as the function of $\log(R/R_c)$ for $n_s = 6$ and various values of h/J below the transition (top of figure) and above the transition (bottom).

shown in Table I. ν is larger than 1 ($\nu = 1.16$ for $n_s = 7$ while the exact value is $\nu = 1$).

The exponent z is a dynamical exponent related to time or energy. When the critical field is approached, the correlation length R_c but also the characteristic time τ diverges (the gap Δ goes to zero) and $\tau \sim \Delta^{-1} \sim R_c^z$. In the renormalization-group transformation the length is changed by a factor n_s, $l' = l/n_s$, and the time is changed by a factor of n_s^z, $t' = t/n_s^z$. $z = 1$ (exact result) means that the time has the same dimension as the space. This exponent z is important as it governs the dynamical critical behavior and the effect of temperature {the temperature effects can no more be neglected when $kT > [h/j - (h/j)_c]^{\phi}$, where the crossover exponent ϕ is equal to the product νz}.[14] The exponent z can be obtained from the recursion relations at the fixed point. In the renormalization-group transformation by forming blocks of spins and reducing the length by a factor of n_s we have also, if we want to stay from the recursion relations at the fixed point. In the renormalization-group transformation by forming blocks of spins and reducing the length by a factor of n_s we have also, if we want to stay in the one parameter space h/J, to impose a dilatation of energy or reduction of time so that the Hamiltonian $H((h/J)^{n+1})$ has the same energy levels as $H((h/J)^n)$. Then

$$E' = n_s^z E(t' = t/n_s^z) \tag{49}$$

where,

$$n_s^{-z} = \frac{J^{(n+1)}}{J^{(n)}} = \frac{h^{(n+1)}}{h^{(n)}} \tag{50}$$

at the fixed point $h/J = (h/J)_c$.

The value of z is obtained by hand for $n_s = 2$ and with the help of the computer for larger values of n_s. The values of z for $n_s = 2, \ldots, 7$ are shown in table I. νz and s should satisfy the scaling law

$$s = \nu z \,. \tag{51}$$

The values of νz are shown in Table I and the scaling law (51) is well satisfied (a sort of self-consistent test of the calculations).

The values of ν and z obtained by this method are not very good. Even with $n_s = 7$ the value of ν is 15% larger than the exact one and z is 15% lower. The critical field is 5% too large. This means that the energy is not rescaled correctly and the first excited level and thus the gap Δ is not represented accurately. This is due to the fact that higher excited states are neglected in the iteration scheme. In the method developed by Friedman[15] and Subarrao[16] all the levels are retained and effective Pauli spin operators are introduced at each step. They get then better results (with $n_s = 3$ from first-order perturbation theory they[15] get $(h/J)_c = 1.01$ and $\nu = 1.13$; z or s were not determined). We shall see however that our approach is much better to describe the ground state and get the "magnetic" exponents $\beta, \eta_x, \ldots$. The values of ν and z plotted versus $1/\sqrt{n_s}$ converge towards the exact values $\nu = z = 1$.

The "magnetic exponents" $\beta, \eta_x, \eta_y, \eta_z$ have been obtained from direct calculations through the renormalization group recursion relations of $\mu_x, \rho_x, \rho_y, \rho_z$ by choosing adequately the sites on the chain to minimize the edge effects of the block partitioning of the method. These values, reported in Table I, are not too far from the exact ones; β, η_x, and η_z tend to the exact values linearly as a function of $1/n_s$ with some oscillation due to the effect of the parity of n_s. For η_y (which is related to η_x through z) the dependence is linear in $1/\sqrt{n_s}$. The exponents should satisfy the scaling laws

$$\eta_x = 2\beta/\nu \,, \tag{52}$$

$$\eta_z = 2(1 + z - 1/\nu) \,, \tag{53}$$

$$\eta_y = \eta_x + 2z \,. \tag{54}$$

The two first equalities can be easily recovered. The third one is obtained as follows: At the fixed point $h/J=(h/J)_c$ the Hamiltonian

$$H=\frac{J}{h}\sum S_i^x S_j^x+\sum S_i^z \tag{55}$$

is invariant but the energies are rescaled $E'=n_s^z E(t'=n_s^{-z}t)$. S_i^y is related to S_i^x.

$$S_i^y=[H,S_i^x]=\frac{\partial}{\partial t}[S_i^x(t)]_{t=0}. \tag{56}$$

Thus if d_x is the dimension of S_i^x ($S_i^{x(n+1)}=n_s^{d_x}S_i^{x(n)}$; $2d_x=\eta_x$) then from (56) $d_y=d_x+z$ and thus Eq. (54) is obtained. The two relations (52) and (54) for η_x and η_y are satisfied as shown in Table I. The relation (53) for η_z is not satisfied (this apparent inconsistency is due to the fact that ν and z are related to a global calculation as η_z has been obtained from the dimension of S_i^z at special site i far from the block edges). As for ν and z it is possible and more easy (if we only want to extract critical indices) to calculate $\beta,\eta_x,\eta_y,\eta_z$ by first extracting at the fixed point the dimensions d_x, d_y, d_z of the operators S_i^x, S_i^y, S_i^z at the well-chosen site i. These dimensions are defined by the relations:

$$S_i^{\alpha(n+1)}=n_s^{d\alpha}S_i^{\alpha(n)}, \tag{57}$$

where

$$n_s^{d\alpha}=(\xi_p^{\alpha(n)})^{-1} \tag{58}$$

with $p=\frac{1}{2}n_s$ [or $\frac{1}{2}(n_s+1)$ if n_s is odd]. At the fixed point $h/J=(h/J)_c$ $\xi_p^{\alpha(n)}$ is independent of n. From renormalization-group arguments it then follows

$$\eta_\alpha=2d_\alpha. \tag{59}$$

The values of d_x,d_y,d_z are reported in Table I and the Eq. (59) is satisfied within a few percent.

Our method gives better results for these "magnetic" critical exponents than for the "thermal" exponent. Already for $n_s=3$ the value 0.18 obtained for β is better than the value 0.21 obtained by Drell *et al.*[2] by use of a sophisticated "variational" renormalization-group method. Furthermore, the "thermal" exponents are easily improved: as shown earlier,[3] for $n_s=2$ and keeping four levels at each iteration, one already obtains the result $s=1$.

VII. CONCLUSION

We have presented here an example of application of a renormalization-group method for quantum spin systems (we have chosen the transverse field Ising model because it is the simplest quantum nontrivial system and because in one dimension almost everything is known exactly). Physical quantities such as magnetization components μ_α, correlation functions ρ_α, ground state, and gap energies can be evaluated at $T=0$. The critical field $(h/J)_c$ can be obtained and the critical behavior in the vicinity of $(h/J)_c$ can be studied. The critical exponents (three of which ν,z,η_x are fundamental) can be extracted either from the analysis of the various quantities close to the critical field or directly through the analysis of the renormalization-group recursion relations near and at the fixed point.

The main conclusion is that taking blocks of two spins in the recursion method gives poor results since edge effects cannot be avoided. Considering blocks of three spins gives significantly improved results. The values of the exponents converge towards exact values when n_s increases. The method is especially good to obtain the ground state, and the "magnetic" exponents are well extracted in contrast to the method of Friedman and Subarrao where on the contrary the "thermal" exponents but not the "magnetic" exponents are correctly obtained. (The "thermal" exponents are related to the structure of the excited levels, the "magnetic" exponents are related to singularities in the ground-state properties).

These results are encouraging and the following program is in progress: We shall (i) improve the calculation for the Kondo-lattice-model Hamiltonian[3] by considering blocks of three spins; (ii) extend the method to the study of time dependent correlation functions and finite temperature effects, by retaining much more low-lying states; (iii) extend the method to other quantum systems (the study of the anisotropic X-Y model in a field is actually done); (iv) extend the method to higher dimensionalities (the transverse Ising model in two dimensions is actually studied); and (v) extend the method to include disorder effects.

ACKNOWLEDGMENTS

Work at Brookhaven was supported in part by the Division of Basic Energy Sciences, U.S. Department of Energy, under Contract No. EY-76-C-02-0016. Work at Stanford was partly supported by the U. S. Army Research Office, Durham, N.C.

*Laboratoire associé au CNRS.
[1]S. Jafarey, R. Pearson, D. J. Scalapino, and B. Stoeckley (unpublished).
[2]S. D. Drell, M. Weinstein, and S. Yankielovicz, Phys. Rev. D 14, 487 (1976).
[3]R. Jullien, J. N. Fields, and S. Doniach, Phys. Rev. Lett. 38, 1500 (1977); Phys. Rev. B 16, 4889 (1977).
[4]R. C. Brower, F. Kuttner, M. Nauenberg, and K. Subbarao, Phys. Rev. Lett. 38, 1231 (1977).
[5]K. G. Wilson, Rev. Mod. Phys. 47, 773 (1975).
[6]P. Pfeuty, Ann. Phys. 57, 79 (1970).
[7]J is simply related by $\bar{\Delta}_{23} = 2J$ to the gap between the ground-state doublet and the following excited states when the fixed point is reached. In fact, one cannot trust the results of the method for the third and following excited states since only the two lowest states are retained at each iteration.
[8]Note that the coordinates $\lambda^{\pm}_{\epsilon_{\pm}} \ldots \epsilon_{n_S}$ have not a definite sign. This yields, through formula (12), an indetermination for the sign of $\langle S^x \rangle$. On the contrary we can see on formula (23) that the sign of $\langle S^z \rangle$ is unambiguous.
[9]We found that the results reported for ρ_y (1) in Ref. 6 were approximate: in fact $-\rho_y$ (1) goes through a maximum after the transition and does not show a peaked maximum at the transition. The dashed curves of Figs. 4 (a)–4(c) have been computed precisely by machine using the exact formulas of Ref. 6.
[10]E. Barouch and B. M. McCoy, Phys. Rev. A 3, 786 (1971).
[11]R. J. Elliott, P. Pfeuty, and C. Wood, Phys. Rev. Lett. 25, 443 (1970).
[12]M. Suzuki, Prog. Theor. Phys. 46, 1337 (1971).
[13]This model first solved by Onsager has led in the last twenty years to further developements well summarized in the book by B. M. McCoy and T. T. Wu, *The Two Dimensional Ising Model* (Harvard University Press, Cambridge, Mass., 1973).
[14]P. Pfeuty, J. Phys. C 9, 3993 (1976).
[15]Z. Friedman, Phys. Rev. Lett. 36, 1326 (1976).
[16]K. Subbarao, Phys. Rev. Lett. 37, 1712 (1976).